Molecular Therapy
Oncology
Original Article

A dual-luciferase bioluminescence system for the assessment of cellular therapies

Alejandro G. Torres Chavez,[1,5] Mary K. McKenna,[1,5] Kishore Balasubramanian,[2] Lisa Riffle,[3] Nimit L. Patel,[3] Joseph D. Kalen,[3] Brad St. Croix,[4] Ann M. Leen,[1] and Pradip Bajgain[4]

[1]Center for Cell and Gene Therapy, Baylor College of Medicine, Houston, TX 77030, USA; [2]Texas A&M Health Science Center School of Medicine, Bryan, TX 77807, USA; [3]Small Animal Imaging Program, Frederick National Laboratory for Cancer Research, Leidos Biomedical Research, Frederick, MD 21702, USA; [4]Tumor Angiogenesis Unit, Mouse Cancer Genetics Program, Center for Cancer Research, National Cancer Institute, Frederick, MD 21702, USA

Bioluminescence imaging is a well-established platform for evaluating engineered cell therapies in preclinical studies. However, despite the discovery of new luciferases and substrates, optimal combinations to simultaneously monitor two cell populations remain limited. This makes the functional assessment of cellular therapies cumbersome and expensive, especially in preclinical *in vivo* models. In this study, we explored the potential of using a green bioluminescence-emitting click beetle luciferase, CBG99, and a red bioluminescence-emitting firefly luciferase mutant, Akaluc, together to simultaneously monitor two cell populations. Using various chimeric antigen receptor T cells and tumor pairings, we demonstrate that these luciferases are suitable for real-time tracking of two cell types using 2D and 3D cultures *in vitro* and experimental models *in vivo*. Our data show the broad compatibility of this dual-luciferase (duo-luc) system with multiple bioluminescence detection equipment ranging from benchtop spectrophotometers to live animal imaging systems. Although this study focused on investigating complex CAR T cells and tumor cell interactions, this duo-luc system has potential utility for the simultaneous monitoring of any two cellular components—for example, to unravel the impact of a specific genetic variant on clonal dominance in a mixed population of tumor cells.

INTRODUCTION

Chimeric antigen receptor (CAR)–modified T cells are now widely used as anticancer agents, particularly for the treatment of $CD19^+$ malignancies,[1,2] and numerous laboratories are exploring new disease targets and interrogating the therapeutic utility of CAR T cells in a range of hematologic and solid tumors.[3–6] Before clinical translation, these novel therapies must undergo extensive *in vitro* (two-dimensional [2D] and 3D) and *in vivo* (animal model) testing, not only to gauge their potency, specificity, and potential efficacy but also to assess the safety of such novel effector molecules.

Although a variety of assays are used to evaluate preclinical endpoints, a mainstay of *in vitro* and small animal model testing involves the genetic modification of effector T cells and target tumor cells with a luciferase enzyme, which enables cell fate monitoring by bioluminescence imaging (BLI).[7,8] Firefly luciferase (FLuc) is the most widely used luciferase to track tumor progression/regression and has made it possible to monitor nonsuperficial tumors in a noninvasive manner. However, the use of a single luciferase means that only one cell population can be analyzed at a time. This precludes simultaneous evaluation of T cell trafficking, localization, infiltration, and expansion and tumor growth/elimination, unless BLI is paired with a secondary and often more sophisticated imaging technologies such as positron emission tomography.[9]

As an alternative, the use of two luciferases to track two cell populations has been explored using various luciferase/substrate pairings in a range of *in vitro* and *in vivo* tumor models.[10–15] Although these studies have established the feasibility of using two-color BLI to monitor two cell populations, their primary focus has been to characterize and test the compatibility of the reported luciferase/substrate pairs. Reports of methodological details and data demonstrating the practical applications of these dual-luciferase (duo-luc) systems, particularly in immunotherapeutic research, is scarce. This precludes nonexpert laboratories from using these luciferases in their research, especially when combined with the limitations such as the need for (1) custom-synthesized substrates that are commercially unavailable or extremely expensive,[10–12,15] and (2) filters/spectral unmixing methods to distinguish the two luciferase signals, which reduce sensitivity and could compromise *in vivo* applications.[12–15]

The goal of the present study was to extensively optimize a previously explored duo-luc system for *in vitro* assays as well as animal models to enable the simultaneous detection of both signals.[10,16] Here, we report on the comprehensive evaluation of a compatible luciferase pair (click beetle green [CBG99],[17,18] and Akaluc[19]), which, upon exposure to substrate (D-Luciferin and AkaLumine-HCl, respectively)

Received 20 September 2023; accepted 5 January 2024;
https://doi.org/10.1016/j.omton.2024.200763.

[5]These authors contributed equally

Correspondence: Pradip Bajgain, PhD, Center for Cancer Research, National Cancer Institute-Frederick, Building 560, Room 32-20, 1050 Boyles St, Frederick, MD 21702, USA.
E-mail: pradip.bajgain@nih.gov

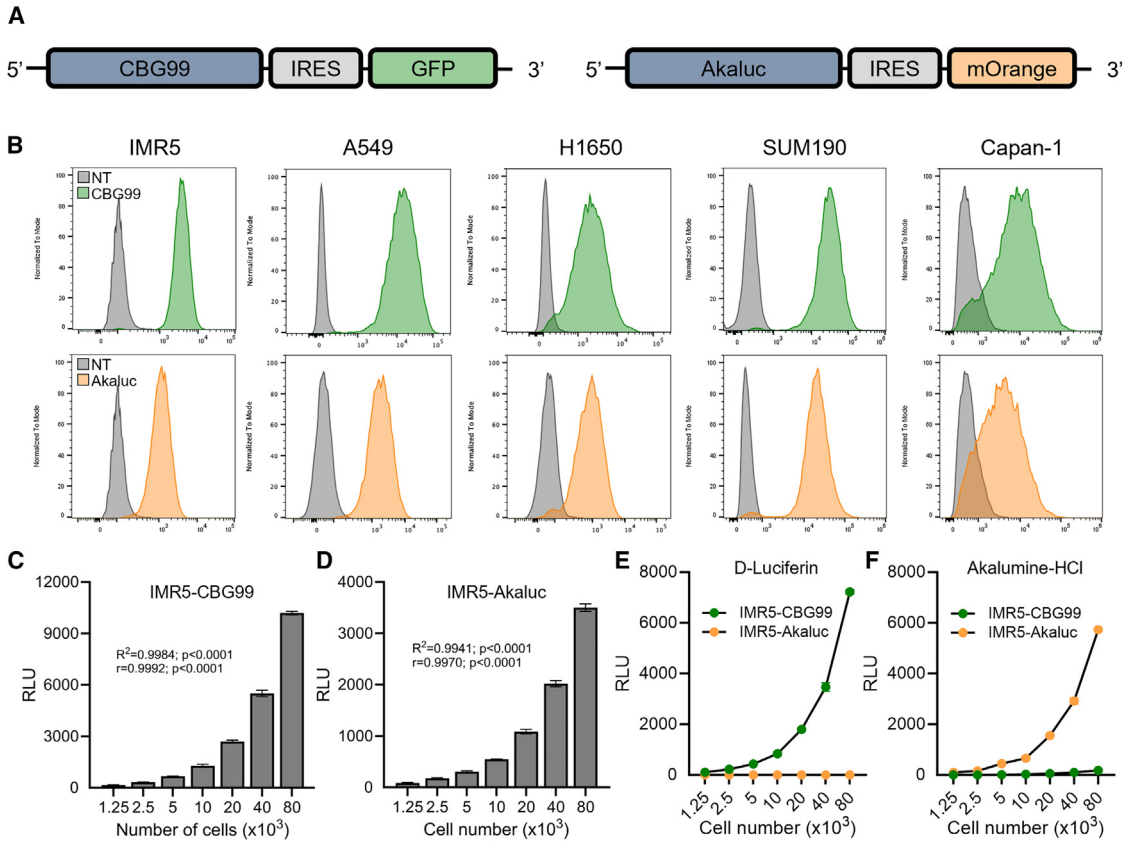

Figure 1. Using CBG99 and Akaluc bioluminescence to track cell behavior *in vitro*

(A) Illustrations of the CBG99 (left) and the Akaluc (right) viral vectors used to engineer cells. (B) Flow cytometry data illustrating the expression of CBG99 indicated by GFP (top row) and Akaluc indicated by mOrange (bottom row) positivity in different tumor cell lines measured after flow cytometric sorting to exclude nontransduced cells. (C) Measurement of CBG99 bioluminescence at different cell densities for IMR5-CBG99 cells. (D) Measurement of Akaluc bioluminescence at various cell densities for IMR5-Akaluc cells. (E) IMR5-CBG99 and IMR5-Akaluc bioluminescence at different seeding densities when exposed to D-Luciferin, captured using the CLARIOstar plate reader with open filter. (F) IMR5-CBG99 and IMR5-Akaluc bioluminescence at different seeding densities when exposed to AkaLumine-HCl, captured using CLARIOstar plate reader with open filter. (C–F) Data shown as mean ± SEM, n = 4.

display unique emission spectra, enabling dual cell tracking.[10,16] We demonstrate not only the broad utility of the system, which is compatible with an array of imaging instrumentation ranging from a benchtop spectrophotometer to *in vivo* imaging systems such as the IVIS Lumina, but also establish the feasibility of using such a platform for modeling complex cell–cell interactions.

RESULTS

Using CBG99 and Akaluc bioluminescence to track cell behavior *in vitro*

CBG99 and Akaluc have been reported to exhibit near-orthogonal specificities for their substrates D-Luciferin and AkaLumine-HCl, respectively.[16,19] This property, in conjunction with the distinct emission spectra (peak emissions approximately 540 nm [CBG99/D-Luciferin] and 650 nm [Akaluc/AkaLumine-HCl]), makes these luciferase-substrate pairs attractive candidates to use in combination for the simultaneous assessment of two different cell populations (i.e., a duo-luc imaging system).[14,19]

To explore the utility of this duo-luc system, we first generated individual retroviral vectors encoding CBG99 and Akaluc to use in our immunotherapeutic CAR T cell:solid tumor models. As a secondary tracker and to facilitate cell sorting, GFP and mOrange fluorescent proteins were co-expressed with CBG99 and Akaluc, respectively, via internal ribosome entry sites (IRESs; Figure 1A). Figure 1B shows that CBG99 and Akaluc can be expressed in tumor cells of various origins, including neuroblastoma (IMR5), lung adenocarcinoma (A549 and H1650), breast cancer (SUM190), and pancreatic cancer (Capan-1). With the exception of Capan-1, all of the cell lines shown in Figure 1B were sorted to enrich for the transduced cells, creating two variants for each cell line with either CBG99 (GFP) or Akaluc (mOrange).

To understand the relationship between CBG99/Akaluc bioluminescence and cell number, we next measured bioluminescence from CBG99- or Akaluc-expressing IMR5 cells seeded at different densities using a plate reader (Figures 1C and 1D). Simple linear regression

modeling and Pearson correlation analysis indicated a strong linear correlation between input IMR5 cell number and bioluminescence (r = 0.9992 and 0.9970 for CBG99 and Akaluc, respectively), a result that was confirmed in a second model using Capan-1 cells and the IVIS Lumina III system to measure bioluminescence (Figures S1A and S1B). We next transitioned from a 2D to a 3D *in vitro* culture system and explored whether these luciferases could be used to label and monitor tumor spheroids. Figures S1C and S1D show imaging (luminescence overlaid well-plate photograph, top) and bioluminescence (bar graphs, bottom) produced by A549 lung adenocarcinoma spheroids captured using the IVIS Lumina III, with a strong correlation between cell number and bioluminescence for both CBG99 (r = 0.9715) and Akaluc (r = 0.9675). Taken together, these data demonstrate that (1) CBG99 and Akaluc can, individually, be used to stably label multiple tumor types, and (2) that bioluminescence signal correlates with cell number and can thus be used to monitor dynamic changes over time.

Next, we explored the feasibility of using these luciferases together to simultaneously track two cell populations by performing substrate cross-reactivity tests in cell culture and in live mice. For *in vitro* testing, we placed IMR5-CBG99 and IMR5-Akaluc cells in culture and exposed them to D-Luciferin and AkaLumine-HCl separately. As shown in Figure 1E, in the presence of D-Luciferin there was a strong and cell number-dependent signal detected from IMR5-CBG99 cells but not from IMR5-Akaluc cells. Similarly, in the presence of AkaLumine-HCl, specific and cell-dependent bioluminescence emanated from IMR5-Akaluc cells (Figure 1F). To test substrate cross-reactivity *in vivo*, we engrafted CBG99$^+$ and Akaluc$^+$ Capan-1 cells on the lower right and left abdomen of NSG mice, respectively (Figure S2A). Subsequently, D-Luciferin or AkaLumine-HCl was injected intraperitoneally and mice were imaged using IVIS Lumina III with an open filter. As shown in Figure S2B, only CBG99$^+$ tumors (lower right abdominal region) produced bioluminescence in mice that received D-Luciferin injection, indicating a low-to-undetectable cross-reactivity of D-Luciferin with Akaluc *in vivo*. Similarly, in the AkaLumine-HCl substrate–injected mice, only the tumor on the lower left abdominal region (Capan-1-Akaluc) produced bioluminescence, whereas no emission was detected from the CBG99$^+$ tumors on the right, indicating the specificity of AkaLumine-HCl with Akaluc and minimal/no cross-reactivity with CBG99 (Figure S2C).

Using CBG99 and Akaluc to monitor effector and target populations *in vitro*

Because our goal was to develop a duo-luc co-culture system in which we could simultaneously track and discriminate between two cell populations based on their spectral emission profiles (Figure S3) (e.g., tumor and effector T cells), next, we explored the feasibility of distinguishing IMR5-CBG99 and IMR5-Akaluc bioluminescence in a 1:1 cell mix following the addition of both of their substrates. The filters used were optimized for their respective emission spectra (CBG99 [540–610 nm] and Akaluc [620–680 nm]) and bioluminescence was captured using a CLARIOstar benchtop microplate reader (Figure S4A). As shown in Figure S4B, use of the CBG99 filter allowed for the detection of bioluminescence from IMR5-CBG99 cells seeded alone or when mixed with IMR5-Akaluc cells, whereas the Akaluc filter (Figure S4C) allowed for the selective detection of bioluminescence produced by IMR5-Akaluc cells (either alone or in a mixed culture) with minimal detection of signal from IMR5-CBG99 cells. The same was true following transition to a 3D model of A549 lung cancer spheroids (Figure S4D), where CBG99 and Akaluc bioluminescence could be readily discerned using the IVIS Lumina III imager and 570 nm and 670 nm filters for CBG99 and Akaluc, respectively (Figures S4E and S4F). An alternative to using discrete IVIS filters to separate bioluminescence from the two luciferases is to capture multiple images using band-pass filters encompassing the emission range of both luciferases and unmix the signals using Living Image software's (Caliper Life Sciences, Hopkinton, MA) spectral unmixing function. This approach enabled successful discrimination of bioluminescence produced by CBG99$^+$ and Akaluc$^+$ A549 cells mixed at different ratios (Figure S5).

We next evaluated whether T cell–mediated antitumor effects could be assessed *in vitro* (Figure 2A). To do this we co-cultured GD2$^+$ IMR5-Akaluc cells, with CBG99-modified T cells with or without a GD2 CAR at various effector-to-target ratios (E:Ts), maintaining the same total cell number in each well. Bioluminescence from both cell populations was captured 48 h later using the aforementioned filters. As shown in Figure 2B, non-CAR-expressing T (NT) cells did not expand and had minimal impact on tumor cell numbers, as evidenced by the Akaluc signal, which remained at levels similar to the control "tumor only" condition (Figure 2B). In contrast, co-culture with CAR$^+$ T cells resulted in T cell expansion (with strong T cell bioluminescence) and potent antitumor effects with a consequent reduction in the tumor signal to near background levels across all E:T ratios (Figure 2C). Using flow cytometry, we confirmed these bioluminescence-based results by quantifying the relative ratio of T cells and tumor cells (representative results, Figure 2D; summary data, Figures 2E and 2F). We performed a second tumor model in which Akaluc$^+$ SUM190 breast cancer cells were co-cultured with CBG99 human epidermal growth factor receptor 2 (HER2) CAR (or control) T cells, with similar outcomes (Figures S6A and S6E). Taken together, these data demonstrate that CBG99 and Akaluc can be used to discriminate between two cell populations and can be used simultaneously to measure and quantify biological outcomes, including, in these examples, the antitumor effects mediated by CAR T cells.

Duo-luc imaging in 3D *in vitro* and xenograft mouse models

To evaluate the utility of the duo-luc system in measuring T cell–mediated antitumor effects in a 3D *in vitro* model, we co-cultured Akaluc$^+$ A549 lung cancer spheroids with CBG99$^+$ NT or HER2 CAR T cells. Akaluc and CBG99 bioluminescence signals were simultaneously captured after 48 h using a plate reader (Figure 3A). As illustrated in Figure 3B, NT cells did not affect the spheroid growth, as indicated by the Akaluc bioluminescence, which was comparable to the untreated control, and no expansion of NT cells was observed.

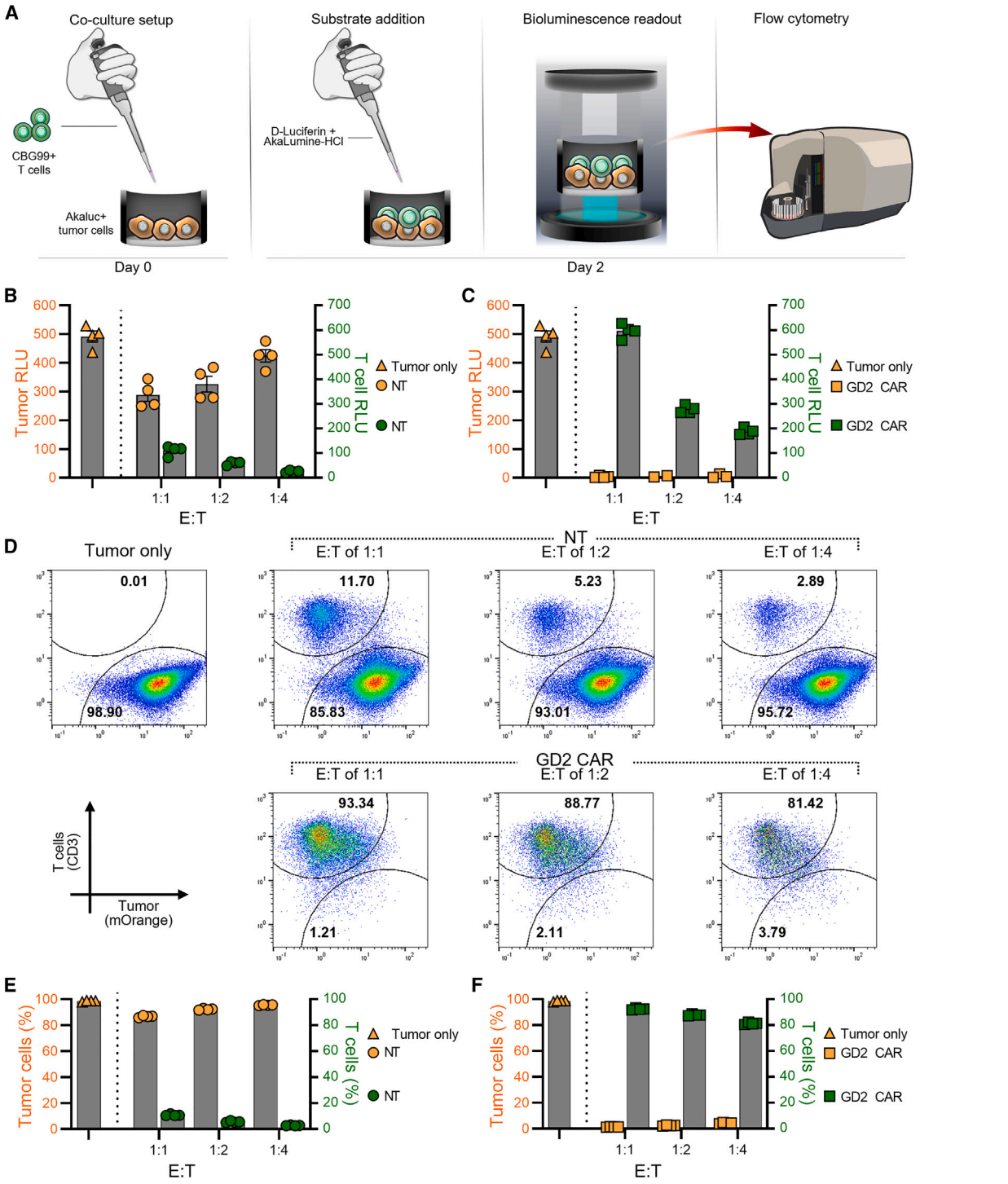

Figure 2. Using CBG99 and Akaluc to monitor effector and target populations *in vitro*

(A) Diagram illustrating the experimental procedure for the 2D co-culture assay using CBG99^{+} T cells and Akaluc^{+} IMR5 tumor cells. (B) Tumor (Akaluc) bioluminescence in absence of T cells (orange triangles), in presence of NT T cells at the indicated E:T ratios (orange circles), and NT cell (CBG99) bioluminescence at the indicated E:T ratios (green circles). (C) Tumor (Akaluc) bioluminescence in absence of T cells (orange triangles), in presence of GD2 CAR T cells at the indicated E:T ratios (orange squares), and GD2 CAR T cell (CBG99) bioluminescence at the indicated E:T ratios (green squares). (B and C) Tumor and T cell bioluminescence signals captured using CLARIOstar plate reader. (D) Flow cytometry plots showing tumor (x axis) and T cell (y axis) populations for a representative donor for each condition in (B) and (C). Numbers indicate percentage of total gated cells. (E and F) Quantitative summary of data shown in (D). (B, C, E, and F) Data shown as mean ± SEM, n = 4.

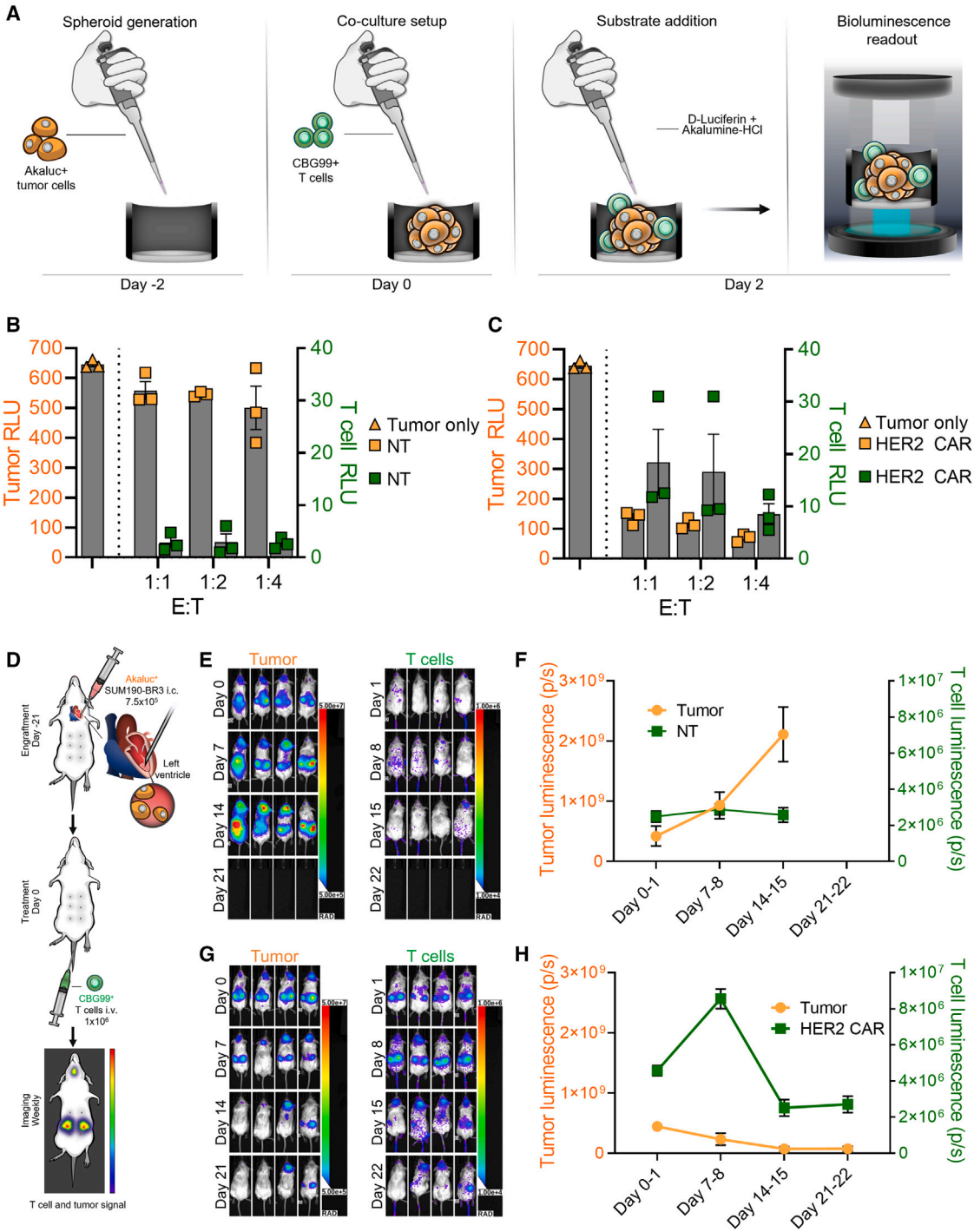

Figure 3. Duo-luc imaging in 3D *in vitro* and xenograft mouse models

(A) Illustration of the experimental procedure for the 3D co-culture assay using CBG99$^+$ T cells and Akaluc$^+$ A549 lung cancer spheroids. (B) A549 tumor spheroids (Akaluc) bioluminescence in absence of T cells (orange triangles), in presence of NT T cells at the indicated E:T ratios (orange squares), and NT cell (CBG99) bioluminescence at the indicated E:T ratios (green squares). (C) Spheroid (Akaluc) bioluminescence in absence of T cells (orange triangles), in presence of HER2 CAR T cells at the indicated E:T ratios (orange squares), and HER2 CAR T cell (CBG99) bioluminescence at the indicated E:T ratios (green squares). (A–C) Tumor and T cell bioluminescence signals captured using

(legend continued on next page)

In contrast, in CAR$^+$ T cell-treated spheroids, the T cell bioluminescence signal increased with a coincidental decrease in tumor bioluminescence, indicating a strong antitumor response (Figure 3C). We obtained similar results in another spheroid model in which Akaluc$^+$ H1650 lung cancer spheroids were treated with CBG99$^+$ NT or HER2 CAR T cells (Figures S7A and S7B).

Finally, we tested the suitability of the duo-luc combination for longitudinal tracking of two cell populations in the same animal. For this, we injected 1×10^6 Akaluc engineered SUM190-BR3 breast cancer cells into the left ventricle of NRG mice to establish metastatic tumors in the brain and other organs. The mice were treated with 1×10^6 CBG99$^+$ NT or HER2 CAR T cells 3 weeks later, and were serially imaged to measure tumor and T cell bioluminescence (Figure 3D). Tumor cells were imaged first, and upon clearance of Akaluc bioluminescence 24 h later (Figure S8), imaging was repeated with D-Luciferin injection to capture T cell bioluminescence. As shown in Figures 3E (representative mice) and 3F (summary data), tumor burden in NT recipient mice continued to increase, indicated by the increase in Akaluc signal over time, and no expansion of NT cells was observed. In contrast, in HER2 CAR T cell–treated mice, the T cell signal initially increased, resulting in tumor control, followed by T cell contraction (Figures 3G, representative mice; 3H, summary data)—dynamic changes that were discernible with the duo-luc system. We confirmed these findings in a second tumor model in which Akaluc$^+$ Capan-1 pancreatic tumors were treated with CBG99$^+$ NT or prostate stem cell antigen (PSCA) CAR T cells (Figures S7C–S7G).

Unlike the *in vitro* assessments, simultaneous monitoring of both T cells and the tumor was not possible in our experimental models due to inefficient CBG99 transduction in T cells, which precluded the use of filters. To test whether simultaneous imaging is feasible with stronger luciferase signals, we implanted Capan-1 tumor cells expressing CBG99 or Akaluc on the opposite sides of NSG mice and subsequently imaged the mice using IVIS Lumina III with open, CBG99, and Akaluc filters (Figure S9A). As shown in Figure S9B, both tumors were detectable with an open filter, whereas only CBG99$^+$ tumor was detected with the CBG99 filter, and only Akaluc$^+$ tumor was detected with the Akaluc filter. This demonstrates that with strong luciferase activity, CBG99- and Akaluc-expressing cells can be imaged simultaneously and distinguished using appropriate filters.

Compatibility with different imaging systems and plate readers

Although our data show that Akaluc and CBG99 can be used to track cells in a range of *in vitro* and *in vivo* studies, it is equally important that such a system is broadly applicable and thus can be easily adopted by the scientific community at large. Therefore, we evaluated the compatibility and reproducibility of results achieved using the duo-luc system with different laboratory equipment. For this investigation, we used the A549 lung cancer spheroid model and measured the bioluminescence produced by CBG99$^+$, Akaluc$^+$, and a 1:1 cell mix using a TECAN Spark benchtop spectrophotometer and IVIS Lumina III. After testing filters ranging from 460 to 700 nm, we identified the 520–590 nm and 655–700 nm filters as optimal for the TECAN, and the 570-nm and 670-nm band-pass filters were found to be ideal for the IVIS. Using the CBG99 filters, both the IVIS and TECAN detected bioluminescence from CBG99$^+$ cells or the mixture of CBG99- and Akaluc-expressing cells (Figures 4A and 4C). Similarly, the Akaluc filter allowed specific detection of Akaluc bioluminescence by both pieces of equipment (Figures 4B and 4D). Both IVIS and TECAN were able to detect cells at all seeding densities; however, bioluminescence at 1×10^3 cells/well or greater was more consistent and distinct from the background luminescence detected from empty wells. These results, in addition to our earlier findings with the benchtop plate reader (Figure S4), confirm the broad utility of the duo-luc system, following the optimization of filter choice and/or bandwidth (for systems with adjustable filters) to ensure that the luciferase signals can be discriminated.

Because the optics and filter configuration often vary between different pieces of equipment, their ability to detect and distinguish the two luciferase signals can also differ. This could result in technical issues such as signal crosstalk between CBG99 and Akaluc filters and underrepresentation of either one of the luciferase signals. We noticed such issues in our A549 spheroids model in the form of a small spillover of CBG99 bioluminescence into the Akaluc filter (Figure 4D), and reduced detection of Akaluc bioluminescence using the TECAN (Figure 4D) in comparison with that observed in the IVIS (Figure 4B). We explored whether the crosstalk between the CBG99 and Akaluc filters could be eliminated during data analysis using algorithm-based correction methods such as the Chroma-Luc Calculator. As shown in Figure S10A, spillover of CBG99 signal was detected in the Akaluc channel, indicated by the bioluminescence detected in the Akaluc filter in the condition with 100% CBG99$^+$ and 0% Akaluc$^+$ A549 cells. Calibration constants for the Chroma-Luc Calculator were calculated using the relative luminescence unit (RLU)s from 100% pure population wells and applied to obtain corrected RLUs, which resolved the crosstalk issue (Figure S10B). The diminished Akaluc detection noted earlier when using the TECAN appears to be a common limitation when using plate readers (in comparison with the IVIS system) because this was also observed with the CLARIOstar (Figure S4). This discrepancy between plate readers and the IVIS may relate to differences in bioluminescence-detection technology (e.g., unlike plate readers, the IVIS uses a supercooled

TECAN plate reader. (D) Illustration of the experimental procedure for the Akaluc$^+$ SUM190-BR3 metastatic breast cancer model in NRG mice. (E) Mice images illustrating tumor imaging (left) and T cell imaging (right) for the NT T cell–treated mice. (F) Quantitative summary of tumor and T cell bioluminescence over time for the NT T cell recipient mice shown in (E). (G) Mice images illustrating tumor imaging (left) and T cell imaging (right) for the HER2 CAR T cell–treated mice. (H) Quantitative summary of tumor and T cell bioluminescence over time for the HER2 CAR T cell recipient mice shown in (G). (E–H) Tumor and T cell bioluminescence were captured 1 day apart using IVIS Spectrum with open filter. (B, C, F, and H) Data presented as mean ± SEM, n = 4.

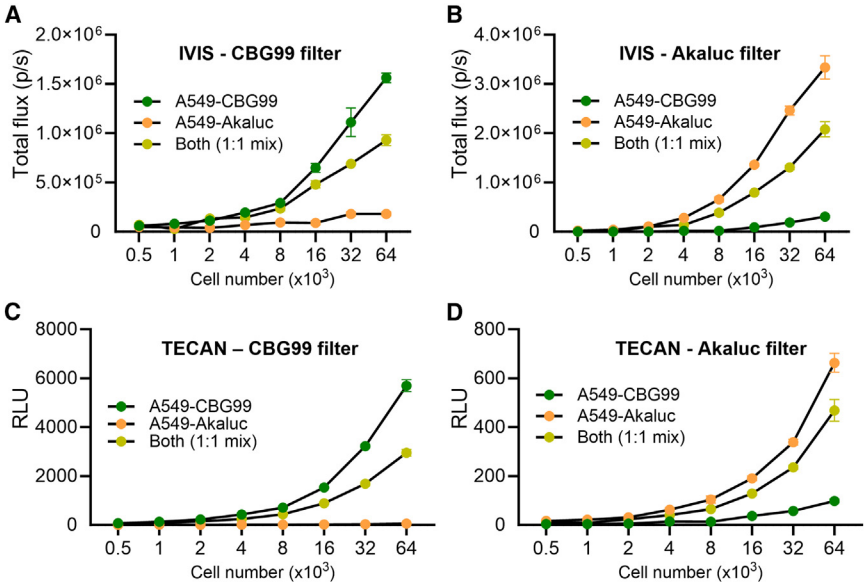

Figure 4. Compatibility with multiple imaging systems and plate readers

(A and B) Bioluminescence signal detected from tumor spheroids generated using A549-CBG99, A549-Akaluc, or a 1:1 mix of both cell types using CBG99-optimized filter (A) or Akaluc-optimized filter (B) after simultaneous addition of D-Luciferin and AkaLumine-HCl. Bioluminescence signals captured using IVIS Lumina III. (C and D) Bioluminescence signal detected from tumor spheroids generated using A549-CBG99, A549-Akaluc, or a 1:1 mix of both cell types using CBG99-optimized filter (A) or Akaluc-optimized filter (B) after simultaneous addition of D-Luciferin and AkaLumine-HCl. Bioluminescence signals captured using TECAN plate reader. (A–D) Data presented as mean ± SEM, n = 4.

charge-coupled device camera) and the filter bandwidths supported by the different pieces of equipment. Such a limitation should be considered when using plate readers and bioluminescence curves (number of cells versus bioluminescence) and should be established for each cell line of interest using appropriate filters for accurate bioluminescence-based prediction of cell numbers.

DISCUSSION

One of the most challenging issues in the field of immunotherapy is to develop preclinical models that recapitulate the human tumor environment for better prediction of the clinical benefit of novel therapeutics.[20] A major bottleneck in overcoming this challenge is the ability to simultaneously assess multiple cell populations of interest. The current work addresses this issue by optimizing a dual reporter BLI system that enabled the simultaneous evaluation of both effector (CAR T cells) and target cells (tumors) in 2D tissue culture, 3D multicellular tumor spheroids that better mimic the physiologic tumor architecture, and traditional *in vivo* animal models.[21,22] This duo-luc system was based on pairing two luciferases (CBG99 and Akaluc) with distinct bioluminescence emission spectra that allowed for their clear detection and discrimination in cells. Since bioluminescence signal strength correlated with cell density, use of this system allowed for the evaluation of dynamic changes in T cell and tumor cell numbers over time and proved reproducible in various solid tumor-CAR T cell models. Furthermore, bioluminescence assessment was compatible with equipment ranging from a benchtop spectrophotometer (e.g., a CLARIOstar, a TECAN) to a small animal optical scanner (e.g., IVIS Spectrum, IVIS Lumina III), supporting the broad utility of this duo-luc system for the assessment of novel immunotherapies through different phases of preclinical development.

Traditional *in vitro* 2D studies examining both T cell and tumor cell behavior are typically performed using either cell surface dyes (e.g., 5-(and-6)-carboxyfluorescein diacetate succinimidyl ester [CFSE], PKH) or ectopically expressed fluorescent molecules such as GFP or mOrange with cell expansion/contraction evaluated and quantified by flow cytometry.[23–27] Three-dimensional tumor spheroids better recapitulate the biophysical characteristics of solid tumors than 2D tumor monolayers and are penetrable by traditional fluorescent imaging.[21,22,28–30] However, greatly increased signal-to-noise ratio and increased sensitivity make BLI a preferred method for detecting dynamic cell population changes.[31–33] Bioluminescence imaging has long been the mainstay for noninvasive interrogation of cellular interactions in living animals, using light emitted from luciferase-expressing reporter cells to track *in vivo* behavior.[34,35] Whole-animal BLI is relatively low cost, high-throughput, useful for serial assessment of *in vivo* cellular events in individual animals, reduces the amount of interanimal variability, and can reduce error, leading to high data quality. Furthermore, because only the live cells with luciferase gene can produce bioluminescence, BLI captures less nonspecific signal (e.g., from tissue and animal feed) than fluorescence imaging, making it the favored approach for *in vivo* imaging.[31,34]

The most widely used luciferase enzyme for optical imaging is firefly luciferase (FLuc), which in the presence of D-Luciferin produces a yellow-green light with a peak emission wavelength of 562 nm. The popularity of FLuc is driven in large part by the lack of endogenous bioluminescent reactions in mammalian tissues, which allows for near background-free imaging.[34,36] However, it is typically used in isolation because of emission overlap with green- and red-emitting luciferases (e.g., enhanced beetle luciferase, red emitting FLuc mutant Ppy RE9, respectively, with peak emission wavelengths of 538 and 620 nm) as well as cross-reactivity with luciferase substrates such as AkaLumine-HCl.[16,37] In the field of CAR T cells, FLuc is used to monitor T cell trafficking, expansion, tumor infiltration, and persistence with localized (e.g., subcutaneous) tumors, whereas antitumor effects are evaluated using caliper measurements.[38,39] However, in the setting of systemic or metastatic tumors, T cell and tumor behavior is often tracked by establishing parallel experiments in

which half contains FLuc-modified T cells and non-gene-modified tumor cells, and the sister experiment is the reverse (FLuc tumor, non-modified CAR T cells). Indeed, for the preclinical studies of a CD19-specific CAR against leukemia, which preceded subsequent clinical trials and ultimately US Food and Drug Administration approval of the clinical product Kymriah, effector T cells were cotransfected to express the CD19 CAR and FLuc to enable assessment of T cell proliferation and persistence in a Nalm-6 xenograft model.[40,41] The antitumor effect of CAR T cells was evaluated in a separate experiment in which FLuc-labeled Nalm-6 tumor-bearing mice were treated with unlabeled CAR T cells.[40] This requirement to track two different parameters in parallel experiments is costly, complex, and cumbersome, limitations that can be readily addressed by using a multireporter system, such as the duo-luc system described here, which pairs two luciferase proteins with divergent bioluminescent emission wavelengths.

When capturing both luciferase signals simultaneously using the CBG99-Akaluc duo-luc system, one limitation is the spectral overlap in the emitted bioluminescence. For example, CBG99 and Akaluc have peak emission wavelengths of approximately 540 and 650 nm, respectively, but their broad emission spectra share some overlap.[16] Thus, for clear discrimination of signals *in vitro* it is important to use the appropriate filters and algorithms to eliminate any residual crosstalk. For example, in our CLARIOstar optimization studies (Figures S4A and S4C), we used 540–610 nm and 620–680 nm bandwidth filters for CBG99 and Akaluc, respectively, and were able to measure both signals individually. Such spectral overlap also complicates *in vivo* imaging because the use of filters to distinguish signals can reduce sensitivity to the extent that the reliable detection of cells with low luciferase activity (e.g., primary T cells, which are smaller and often difficult to transduce) is precluded. To ensure maximum sensitivity, in the present study we chose to capture the two luciferase signals on consecutive days but without filters. For simultaneous *in vivo* imaging, strategies to increase bioluminescence output, particularly of the cells with low luciferase activity, like vector optimization, enrichment of luciferase expressing cells (e.g., flow cytometric sorting), and substrate dose escalation, should be considered.

Although the present work has focused on assessing CAR-T cell–tumor cell interactions, the duo-luc system could be used in a variety of cell-based systems. For example, to improve effector function, proliferative capacity and *in vivo* persistence of effector T cells in the immune suppressive solid tumor microenvironment, our group and others have investigated the infusion of a combination of CARs targeting CD19 and CD22 or combining a CAR with a secondary ectopic molecule designed to subvert the inhibitory effects of molecules such as interleukin-4 (IL-4) and FasL.[38,42–44] The duo-luc system can be used to monitor the *in vivo* behavior and interaction of such complimentary T cell products. Another utility of this system is in studies investigating the therapeutic efficacy of cellular or other immunotherapies such as checkpoint inhibitors and antibody-drug conjugates against two tumor variants (e.g., antigen "high" versus "low" tumor cells), which are differentially luciferase labeled. The platform can be further extended by combining these luciferase molecules with other imaging constructs, in which the secondary construct is a far-red/near-infrared emitting luciferase or fluorescent protein, enabling monitoring of a third cellular component.

In summary, we have optimized a duo-luc BLI system for simultaneous monitoring of two cell populations in the same experimental system and optimized it for the functional assessment of cellular therapies. This platform has potential utility for the simultaneous monitoring of any two cellular components beyond its applications in cell therapy research—for example, to unravel the impact of a specific genetic variant on clonal dominance in a mixed population of tumor cells. Unlike previously described duo-luc systems, the CBG99-Akaluc pair does not require custom-synthesized or expensive substrates because both D-Luciferin and AkaLumine-HCl are readily available commercially, and is amenable for the development of both simultaneous and sequential BLI strategies. These features, in combination with its compatibility with multiple BLI equipment, makes the CBG99-Akaluc duo-luc system easily adoptable by the broad scientific community to facilitate research in immunotherapy and beyond.

MATERIALS AND METHODS

Cell lines

All of the cell lines used in the study (293T, Capan-1, A549, H1650, SUM190, and IMR5) were obtained from the American Type Culture Collection (Rockville, MD) between the years 2012 and 2014, and passages between 8 and 24 were used in the experiments. Cell lines 293T and Capan-1 were cultured in complete Iscove's modified Dulbecco's medium (IMDM, Gibco BRL Life Technologies, Gaithersburg, MD, catalog no. 12440-046) supplemented with 10% heat-inactivated fetal bovine serum (FBS) (Hyclone, Waltham, MA, catalog no. SH30088.02HI) and 2 mM GlutaMAX (Gibco BRL Life Technologies, catalog no. 35050-061). A549, H1650, and IMR5 were cultured in DMEM medium (Cytiva-Hyclone, Marlborough, MA, catalog no. SH30081.01) supplemented with 10% heat-inactivated FBS. SUM190 cells were kindly provided by Dr. Patricia Steeg (Women's Malignancies Branch, National Cancer Institute) and cultured in Ham's F-12 medium (Mediatech, Manassas, VA, catalog no. 10-080-CV) supplemented with 1× insulin-transferrin-selenium-ethanolamine supplement (Gibco BRL Life Technologies, catalog no. 51500056), 1 μg/mL hydrocortisone (Millipore Sigma, Burlington, MA, catalog no. H0396), 10 mM HEPES (Gibco BRL Life Technologies, catalog no. 15630080), 10 nm triiodo thyronine (R&D Systems, Minneapolis, MN, catalog no. 6666/50), and 1 g/L BSA (Gibco BRL Life Technologies, catalog no. 15260037). All of the cell lines were maintained in a humidified incubator containing 5% CO_2 at 37°C. Mycoplasma testing was performed on cell culture supernatants using the MycoAlert Mycoplasma Detection Kit (Lonza, Rockland, ME, catalog no. LT07-418), and all of the cell lines were confirmed to be negative. The identity of all of the cell lines was validated by short tandem repeat profiling, performed by the University of Arizona Genetics Core or the MD Anderson Cancer Center Cytogenetics and Cell Authentication Core.

Spheroids generation

The 96-well black with clear flat-bottom tissue culture–treated plates (Corning, Corning, NY, catalog no. 3904) were coated with 45 μL of 1% (w/v) agarose (Thermo Fisher Scientific, Pittsburgh, PA, catalog no. BP160-500). Serial dilutions of Akaluc- or CBG99-transduced tumor cells were resuspended in 55 μL of T cell medium and seeded in a final volume of 100 μL. The plates were incubated at 37°C for 48 h to allow spheroid formation and subsequently used in experiments.

Generation of retroviral constructs and retroviral supernatant

To generate the CBG99 vector, we incorporated a synthesized linear DNA fragment (IDT DNA Technologies, Coralville, IA) encoding CBG99 enzyme into an SFG retroviral vector backbone upstream of the GFP tag linked by an IRES sequence. To generate the Akaluc vector, the FLuc mutant Akaluc insert (IDT DNA Technologies) was incorporated into the SFG retroviral vector backbone, which also contained the fluorescent marker mOrange linked by an IRES sequence downstream of the insertion site. The PSCA,[39] HER2,[45] and GD2[46] specific CARs used in the study have been published previously and were expressed in T cells using the SFG vector. The SFG retroviral vector was provided by Dr. Cliona Rooney and was originally received from Dr. Richard Mulligan.[47] Retroviral supernatant for all constructs was generated by the transfection of 293T cells, as described previously.[43] Briefly, 3.5×10^6 293T cells were plated in 100-mm tissue culture–treated dishes (Falcon-A Corning Brand, Glendale, AZ, catalog no. 353003) in 10 mL complete IMDM medium. A day later, cells were transfected with PegPam-e, RD114, and the DNA construct loaded into GeneJuice Transfection Reagent (Millipore, Burlington, MA, catalog no. 70967). All of the virus supernatants were collected at 48 and 72 h, pooled together, sterile filtered using 0.2-μm filters (Pall Corporation, Port Washington, NY, catalog no. 4652) and stored at −80°C until transduction.

Transduction of tumor cell lines

We generated tumor cell lines (Capan-1, A549, H1650, SUM190, and IMR5) that stably expressed CBG99 or Akaluc luciferases following retroviral transduction as described previously.[44] Briefly, retroviral supernatant was plated in a nontissue culture–treated 24-well plate (1 mL/well), which was precoated with RetroNectin–recombinant fibronectin fragment (FN CH-296) (Takara Shuzo, Otsu, Japan, catalog no. T100B) and centrifuged at 2,000 × *g* for 90 min. Tumor cells (1.5×10^5 per well) were added to the plates and centrifuged at 400 × *g* for 5 min, then transferred to a 37°C, 5% CO_2 incubator.

Donor and generation of CAR T cells

Peripheral blood for T cell generation was obtained from healthy volunteers under a protocol approved by the institutional review board (Baylor College of Medicine) or from the research donor program (National Cancer Institute at Frederick). PBMCs were isolated from the donor blood by density gradient centrifugation using Lymphoprep (Serumwerk Bernburg AG for Alere Technologies AS, Oslo, Norway, catalog no. 1114544). To generate CAR T cells, 1×10^6 PBMCs were plated in each well of a nontissue culture–treated 24-well plate (Falcon-A Corning Brand, catalog no. 351147) that had been precoated with the CD3-specific antibody OKT3 (1 mg/mL) (Ortho Biotech, Bridgewater, NJ) and CD28 (1 mg/mL) (Becton Dickinson, Mountain View, CA, catalog no. 555725). Cells were cultured in complete media (RPMI 1640, Cytiva-Hyclone, Marlborough, MA, catalog no. SH30096.01) containing 45% Clicks medium (Irvine Scientific, Santa Ana, CA, catalog no. 9195), 10% FBS, and 2 mM L-GlutaMAX), which was supplemented with recombinant human IL-2 (50 U/mL, National Institutes of Health, Bethesda, MD) on day 1. On day 3 post-OKT3/CD28 T-blast generation, 1 mL of retroviral supernatant was added to a 24-well nontissue culture–treated plate precoated with RetroNectin and centrifuged at 2,000 × *g* for 90 min. OKT3/CD28-activated T cells (0.2×10^6/mL) were resuspended in complete media supplemented with IL-2 (100 U/mL) and then added to the wells and centrifuged at 400 × *g* for 5 min. To generate CAR- and CBG99-expressing cells, activated T cells were transduced as described above, first with the CAR construct (on day 3) and then with CBG99 on day 4. Transduction efficiency was measured 3 days after the last transduction by flow cytometry.

Flow cytometry and cell sorting

Luciferase transduction of tumor cells was analyzed by flow cytometry 1 week posttransduction. Cells were subsequently sorted based on GFP or mOrange expression to exclude nontransduced tumor cells using a Sony SH800Z cell sorter (Sony Biotechnology, San Jose, CA), FACS Aria II (Beckton Dickinson), or Symphony S6 (Beckton Dickinson) cell sorters. Sorted cells were cultured for 2 weeks to obtain sufficient numbers to prepare a cryopreserved bank for all of the experiments. GFP/mOrange expression was assessed by flow cytometry and confirmed to be ∼100% on the day of cryopreservation.

CAR expression by T cells after transduction was measured by flow cytometry. PSCA and GD2 CARs were detected using goat anti-human F(ab′)2 antibody conjugated with Alexa Fluor 647 (Jackson ImmunoResearch Laboratories, West Grove, PA, catalog no. 109-606-097). HER2 CAR was detected using a chimeric Erb2-Fc fusion protein (R&D Systems, catalog no. 1129-ER-050) with Alexa Fluor 647 anti-Fc antibody (Southern Biotech, Birmingham, AL, catalog no. 2014-31). Cells were stained with saturating amounts of antibody (∼5 μL) for 20 min at 4°C, washed with 1× Dulbecco's PBS (DPBS; Sigma-Aldrich, St. Louis, MO, catalog no. D8537), and then acquired on the Gallios Flow Cytometer (Beckman Coulter, Brea, CA) or LSR II SORP (Becton Dickinson). Analysis was performed using Kaluza Flow analysis software (Beckman Coulter) version 2.1 or FlowJo version 10.9.0 (Becton Dickinson).

Luciferase substrates

The substrate for CBG99 luciferase, D-Luciferin (PerkinElmer, Boston, MA, catalog no. 122799), was prepared by dissolving the lyophilized substrate in sterile 1× DPBS to achieve the final concentration of 15 mg/mL (47.1 mM). AkaLumine-HCl (Sigma-Aldrich, catalog no. 808350), the substrate for Akaluc, was dissolved in sterile H_2O (Corning, catalog no. 46-000-CV) to prepare a 8.5 mg/mL stock solution (25 mM), which was then diluted with 0.9% NaCl (Millipore Sigma, catalog no. S9625) to generate a working solution with a

concentration of 1.7 mg/mL (5 mM). Both substrates were aliquoted and stored at −20°C until use.

Bioluminescence signal at different cell densities

To evaluate the correlation between bioluminescence and cell number, serial dilutions of CBG99-transduced tumor cells were plated in 96-well black flat-bottom tissue culture–treated plates (Corning, catalog no. 3603) with a final volume of 200 μL per well of tumor cell medium. The plates were incubated for 1 h at 37°C, and D-Luciferin solution was added to each well at the final concentration of 15 μg/mL. Bioluminescence signal was captured with an open emission filter using a bioluminescence capable microplate reader/imager. Akaluc-labeled tumor cells were also seeded at different densities as described above. Subsequently, AkaLumine-HCl solution was added to each well (final concentration of 1.7 μg/mL) and bioluminescence was captured as previously described. Similar experiments were performed with other CBG99- or Akaluc-labeled tumor cell lines as well as 3D tumor spheroid models used in the study. Bioluminescence for IMR5 cells was captured using CLARIOstar microplate reader (BMG LABTECH, Cary, NC), Capan-1 cells were obtained using IVIS Lumina III (PerkinElmer), and A549 spheroids measured by IVIS Lumina III or TECAN Spark microplate reader (Tecan Group, Männedorf, Switzerland), depending on the experiment. Capan-1 and A549 spheroid images captured by IVIS Lumina III were analyzed using Living Image software (Caliper Life Sciences).

Substrate cross-reactivity assay

To assess the cross-reactivity of CBG99 with AkaLumine-HCl and Akaluc with D-Luciferin, serial dilutions of CBG99- and Akaluc-transduced IMR5 cells were plated in 96-well black flat-bottom tissue culture–treated plates (Corning) in a final volume of 200 μL per well of tumor cell medium. After 1 h incubation at 37°C, D-Luciferin (final concentration of 15 μg/mL) was added to both CBG99- and Akaluc-transduced tumor cells and bioluminescence signal was captured with an open emission filter using the CLARIOstar microplate reader. A different set of plates seeded with CBG99- and Akaluc-transduced IMR5 cells was used to test AkaLumine-HCl cross-reactivity. After the addition of AkaLumine-HCl (final concentration of 1.7 μg/mL), bioluminescence was captured as previously described. Substrate cross-reactivity of A549 spheroids was performed using a similar experimental setup. A549 bioluminescence was captured using IVIS Lumina III and data were analyzed using Living Image software (Caliper Life Sciences). To assess substrate cross-reactivity *in vivo*, 6- to 8-week-old female and male NSG mice were engrafted with 5×10^6 CBG99$^+$, Capan-1, and 5×10^6 Akaluc$^+$ Capan-1, on the lower right and lower left abdomen, respectively. Ten minutes after intraperitoneal injection of D-Luciferin (100 μL of 15 mg/mL stock solution [1.5 mg per mouse]) or AkaLumine-HCl (100 μL of 5 mM AkaLumine-HCl solution [0.17 mg per mouse]), mice were imaged using IVIS Lumina III (PerkinElmer). Images were captured using open filter.

Differentiation of bioluminescence signals using filters

To identify the ideal filters to differentiate CBG99 and Akaluc bioluminescence, a serial dilution of CBG99- or Akaluc-transduced tumor cells separately, or both cell types mixed at a ratio of 1:1, were plated in 96-well black flat-bottom tissue culture–treated plates (Corning) with a final volume of 200 μL per well of tumor cell medium. The plate was incubated for 1 h at 37°C. A substrate solution containing D-Luciferin and AkaLumine-HCl was prepared and was added to each tumor well (D-Luciferin final concentration of 15 μg/mL, AkaLumine-HCl final concentration of 1.7 μg/mL). Bioluminescence was captured using CLARIOstar plate reader with filter bandwidths randing from 450 to 750 nm. Filter bandwidths of 540–610 nm and 620–680 nm were identified as ideal ranges for the detection of CBG99 and Akaluc bioluminescence signals while preventing the detection of the opposite luciferase signal output. These filters were used in all subsequent experiments requiring the discrimination of CBG99 and Akaluc bioluminescence. Ideal CBG99 and Akaluc filters when using the TECAN plate reader and the IVIS Lumina III were also identified using a similar approach. The 520–590 and 655–700 nm filters were optimal for the TECAN, whereas the 570 and 670 nm band-pass filters were found to be ideal for the IVIS to distinguish bioluminescence from the two luciferases. Analysis of IVIS Lumina III–captured images were performed using Living Image software (Caliper Life Sciences).

Filter crosstalk correction and spectral unmixing

The use of filters to distinguish CBG99 and Akaluc bioluminescence can sometimes result in crosstalk between the two filters (depending on the equipment used to capture bioluminescence signals). To evaluate whether crosstalk can be corrected using spectral unmixing, CBG99$^+$ and Akaluc$^+$ A549 cells were mixed at different ratios and seeded in 96-well black, flat-bottom tissue culture–treated plates coated with 45 μL of 1% (w/v) agarose. After overnight incubation to allow spheroid formation, D-Luciferin, AkaLumine-HCl, or a mix of both substrates were added to the wells at the concentrations used in the substrate cross-reactivity assay. Bioluminescence signals were captured using the TECAN plate reader without any filters (open filter), or with 520–590 and 655–700 nm filters. A replicate plate was similarly imaged using IVIS Lumina III without or with 520-, 570-, 620-, 670-, 710-, 790-, and 845-nm band-pass filters. The TECAN data were analyzed using Chroma-Luc Calculator version 1.0 (Promega Corporation, Madison WI) to calculate the corrected bioluminescence values. IVIS data were analyzed and spectral unmixing was performed using the built-in functions of the Living Image software (Caliper Life Sciences).

Luciferase-based cytotoxicity assay

Cytotoxicity of CAR engineered T cells was tested using T cell:tumor co-culture experiments in which CBG99-labeled T cells were challenged with Akaluc-transduced tumor cells. Tumor cells 5×10^3 were seeded in 96-well black flat-bottom tissue culture–treated plates (Corning) in 100 μL of T cell medium. After 1 h incubation at 37°C, nontransduced or CAR-transduced T cells were resuspended in 100 μL of T cell medium and added to the tumor wells, resulting in an E:T of 1:1, 1:2, and 1:4. The plates were incubated at 37°C. Two days later, a premixed solution of D-Luciferin and AkaLumine-HCl was added to each well (D-Luciferin final concentration of 15 μg/mL, AkaLumine-HCl final concentration of 1.7 μg/mL), and both

T cell (CBG99) and tumor (Akaluc) bioluminescence signals were captured using the equipment-appropriate filters described above. In some experiments, cells were collected from the wells for flow cytometry after capturing bioluminescence data. T cells were resuspended in culture medium by gentle pipetting and transferred to flow cytometry sample tubes (Falcon-A Corning Brand, catalog no. 352052). Tumor cells left in the co-culture wells were detached by incubating at 37°C after adding 50 μL TrypLE Express (Gibco BRL Life Technologies, catalog no. 12605010). Culture medium of 100 μL was added after incubation, and tumor cells were resuspended by pipetting and transferred to sample tubes containing T cells from the same wells. Samples were stained with allophycocyanin-conjugated anti-human CD3 antibody (BioLegend, San Diego, CA, catalog no. 300412) to distinguish T cells from tumor cells. mOrange expressed with Akaluc was used as the marker for tumor cells. Before sample analysis, 7-AAD (BD Biosciences, catalog no. 51-68981E) was added to exclude dead cells. Data were acquired using MACSQuant Analyzer 16 flow cytometer (Miltenyi Biotec, Gaithersburg, MD) and analysis was performed in FlowJo version 10.9.0 (Becton Dickinson).

In vivo studies

To monitor tumor growth and T cell activity in the same mice, a brain-metastatic breast cancer model was used under a protocol approved by the National Cancer Institute Institutional Animal Care and Use Committee (ASP no. 20–078). Ultrasound-guided injection of 7.5×10^5 Akaluc-labeled SUM190-BR3 tumor cells into the left ventricle of 6- to 8-week-old female NRG mice (NOD.Cg-Rag1tm1Mom Il2rgtm1Wjl/SzJ, Jackson Laboratory strain no. 007799) was performed to establish metastatic tumors. Tumor burden was monitored weekly by bioluminescene imaging using IVIS Spectrum optical scanner (PerkinElmer) 10 min after intraperitoneal injection of 100 μL 5 mM AkaLumine-HCl solution (0.17 mg/mouse). Three weeks after tumor injection, mice were grouped into treatment groups and received 1×10^6 CBG99-modified NT or HER2 CAR-transduced T cells intravenously via tail vein injection. Initial T cell bioluminescence was captured 1 day post-T cell administration and was assessed weekly thereafter using IVIS Spectrum 10 min following the intraperitoneal injection of 100 μL stock (15 mg/mL) D-Luciferin solution (1.5 mg/mouse). Unlike *in vitro* experiments, tumor and T cell bioluminescence were captured on separate days using open emission filters for maximum sensitivity because simultaneous imaging with filters was not possible, particularly for T cells due to the small number of cells injected and poor CBG99 transduction. The 1-day gap between imaging sessions allowed for the clearance of Akaluc/AkaLumine-HCl bioluminescence before CBG99/D-Luciferin bioluminescence capture. Data were analyzed using Aura version 4.0.7 (Spectral Instruments Imaging, Tucson, AZ). Capan-1 tumor study was performed at Baylor College of Medicine according to a protocol approved by the Baylor College of Medicine Institutional Animal Care and Use Committee (protocol no. AN-5639). A total of 5×10^6 Akaluc$^+$ Capan-1 tumor cells were implanted subcutaneously into the left flank of 6- to 8-week-old female and male NSG mice (NOD.Cg-Prkdc^{scid} IL-2rg^{tm1Wjl}/SzJ, Jackson ImmunoResearch Laboratories). Once the tumor reached a size of approximately 140 mm^3 (approximately 4 weeks after injection), an initial bioluminescence measurement was taken. Animals were then intravenously injected with 5×10^6 CBG99$^+$ NT or PSCA CAR T cells. Tumor growth and antitumor activity were monitored using BLI as well as caliper measurement. Tumor dimensions obtained by caliper measurements were used to calculate tumor volume using the formula: length × width × width/2. Bioluminescence imaging was performed weekly using IVIS Lumina III (PerkinElmer) 10 min after intraperitoneal injection of 100 μL 5 mM AkaLumine-HCl solution (0.17 mg/mouse). Imaging was repeated the next day 10 min after an intraperitoneal injection of 100 μL stock (15 mg/mL) D-Luciferin (1.5 mg/mouse) to monitor T cell expansion and persistence. Mice were euthanized once the tumor volume reached the protocol limit (1,500 mm^3) or in the event of tumor ulcerations that grew >2 mm in diameter despite treatment or recurred. Mice were monitored for manifestations of toxicities by research personnel as well as Baylor College of Medicine veterinary staff, including measuring body weight and observing visual symptoms of illness (e.g., ruffled coat, hair loss, skin redness). The images were analyzed using Living Image software, version 4.7.4 (PerkinElmer).

Simultaneous *in vivo* imaging

Simultaneous capture of both luciferase signals in mice was tested using NSG mice Capan-1 subcutaneous tumor models in NSG mice. The 6- to 8-week-old female and male mice were engrafted with 5×10^6 CBG99$^+$ Capan-1 and 5×10^6 Akaluc$^+$ Capan-1 in a 100-μL solution containing equal volumes of PBS and Matrigel (Corning, catalog no. 356234), on the lower right and lower left abdomen, respectively. D-Luciferin and AkaLumine-HCl were premixed and injected intraperitoneally at the doses used for *in vivo* tumor studies 10 min before imaging using IVIS Lumina III. Images were captured using open filter to detect both luciferase signals, a 570-nm band-pass filter to detect CBG99-only signal, and a 670-nm band-pass filter to detect Akaluc-only bioluminescence.

Statistical analysis

Data are reported as average ± SEM. Correlation between cell numbers and bioluminescence output was determined by simple linear regression modeling and Pearson correlation analysis in the GraphPad Prism software version 9.5.1 (GraphPad Software). Statistical differences between groups were analyzed by Student's t test and one-way or two-way ANOVA in GraphPad Prism. p value < 0.05 was regarded as statistically significant.

DATA AND CODE AVAILABILITY

The datasets generated and/or analyzed during the present study are included within the article and its supplemental information files. Additional/raw data generated during the study are available from the corresponding author upon reasonable request.

SUPPLEMENTAL INFORMATION

Supplemental information can be found online at https://doi.org/10.1016/j.omton.2024.200763.

ACKNOWLEDGMENTS

This study was supported by NIH grant P01 CA094237, NIH grant P50 CA126752, and Center for Cancer Research (CCR), part of NCI's intramural research program, NIH, Department of Health and Human Services (DHHS). The content of this publication does not necessarily reflect the views or policies of the DHHS nor does mention of trade names, commercial products, or organizations imply endorsement by the US government. We acknowledge the Texas Children's Hospital Small Animal Imaging Facility, the shared resources support from the Dan L. Duncan Comprehensive Cancer Center (P30 CA125123), the NCI Small Animal Imaging Program, and the CCR-Frederick/Cancer Innovation Laboratory Flow Cytometry Core for support. We also thank Walter Mejia for the illustrations and artwork used in the manuscript figures.

AUTHOR CONTRIBUTIONS

A.M.L. and P.B. conceived and designed the project. A.G.T.C., M.K.M., B.S.C., A.M.L., and P.B. planned the experiments. A.G.T.C., M.K.M., K.B., L.R., N.L.P., and P.B. performed the experiments and data analysis. J.D.K. oversaw the *in vivo* imaging studies and edited the manuscript. A.M.L. and P.B. wrote the manuscript. All of the authors reviewed and approved the submission.

DECLARATION OF INTERESTS

A.M.L. is a consultant for and an equity holder of AlloVir, and an equity holder of Marker Therapeutics. All of the other authors declare no competing interests.

REFERENCES

1. Strati, P., Gregory, T., Majhail, N.S., and Jain, N. (2023). Chimeric Antigen Receptor T-Cell Therapy for Hematologic Malignancies: A Practical Review. JCO Oncol. Pract. *19*, 706–713.
2. Denlinger, N., Bond, D., and Jaglowski, S. (2022). CAR T-cell therapy for B-cell lymphoma. Curr. Probl. Cancer *46*, 100826.
3. Leung, W.K., Ayanambakkam, A., Heslop, H.E., and Hill, L.C. (2022). Beyond CD19 CAR-T cells in lymphoma. Curr. Opin. Immunol. *74*, 46–52.
4. Pasqui, D.M., Latorraca, C.D.O.C., Pacheco, R.L., and Riera, R. (2022). CAR-T cell therapy for patients with hematological malignancies. A systematic review. Eur. J. Haematol. *109*, 601–618.
5. Wagner, J., Wickman, E., DeRenzo, C., and Gottschalk, S. (2020). CAR T Cell Therapy for Solid Tumors: Bright Future or Dark Reality? Mol. Ther. *28*, 2320–2339.
6. Yeku, O., Li, X., and Brentjens, R.J. (2017). Adoptive T-Cell Therapy for Solid Tumors. Am. Soc. Clin. Oncol. Educ. Book. *37*, 193–204.
7. Fu, X., Tao, L., Rivera, A., Williamson, S., Song, X.T., Ahmed, N., and Zhang, X. (2010). A simple and sensitive method for measuring tumor-specific T cell cytotoxicity. PLoS One *5*, e11867.
8. Kiesgen, S., Messinger, J.C., Chintala, N.K., Tano, Z., and Adusumilli, P.S. (2021). Comparative analysis of assays to measure CAR T-cell-mediated cytotoxicity. Nat. Protoc. *16*, 1331–1342.
9. Skovgard, M.S., Hocine, H.R., Saini, J.K., Moroz, M., Bellis, R.Y., Banerjee, S., Morello, A., Ponomarev, V., Villena-Vargas, J., and Adusumilli, P.S. (2021). Imaging CAR T-cell kinetics in solid tumors: Translational implications. Mol. Ther. Oncolytics *22*, 355–367.
10. Zambito, G., Hall, M.P., Wood, M.G., Gaspar, N., Ridwan, Y., Stellari, F.F., Shi, C., Kirkland, T.A., Encell, L.P., Löwik, C., and Mezzanotte, L. (2021). Red-shifted click beetle luciferase mutant expands the multicolor bioluminescent palette for deep tissue imaging. iScience *24*, 101986.
11. Su, Y., Walker, J.R., Park, Y., Smith, T.P., Liu, L.X., Hall, M.P., Labanieh, L., Hurst, R., Wang, D.C., Encell, L.P., et al. (2020). Novel NanoLuc substrates enable bright two-population bioluminescence imaging in animals. Nat. Methods *17*, 852–860.
12. Stowe, C.L., Burley, T.A., Allan, H., Vinci, M., Kramer-Marek, G., Ciobota, D.M., Parkinson, G.N., Southworth, T.L., Agliardi, G., Hotblack, A., et al. (2019). Near-infrared dual bioluminescence imaging in mouse models of cancer using infraluciferin. Elife *8*, e45801.
13. Cavnar, S.P., Rickelmann, A.D., Meguiar, K.F., Xiao, A., Dosch, J., Leung, B.M., Cai Lesher-Perez, S., Chitta, S., Luker, K.E., Takayama, S., and Luker, G.D. (2015). Modeling selective elimination of quiescent cancer cells from bone marrow. Neoplasia *17*, 625–633.
14. Mezzanotte, L., Que, I., Kaijzel, E., Branchini, B., Roda, A., and Löwik, C. (2011). Sensitive dual color in vivo bioluminescence imaging using a new red codon optimized firefly luciferase and a green click beetle luciferase. PLoS One *6*, e19277.
15. Branchini, B.R., Southworth, T.L., Fontaine, D.M., Kohrt, D., Florentine, C.M., and Grossel, M.J. (2018). A Firefly Luciferase Dual Color Bioluminescence Reporter Assay Using Two Substrates To Simultaneously Monitor Two Gene Expression Events. Sci. Rep. *8*, 5990.
16. Zambito, G., Gaspar, N., Ridwan, Y., Hall, M.P., Shi, C., Kirkland, T.A., Encell, L.P., Löwik, C., and Mezzanotte, L. (2020). Evaluating Brightness and Spectral Properties of Click Beetle and Firefly Luciferases Using Luciferin Analogues: Identification of Preferred Pairings of Luciferase and Substrate for In Vivo Bioluminescence Imaging. Mol. Imag. Biol. *22*, 1523–1531.
17. Wood, K.V., Lam, Y.A., Seliger, H.H., and McElroy, W.D. (1989). Complementary DNA coding click beetle luciferases can elicit bioluminescence of different colors. Science *244*, 700–702.
18. Zhao, H., Doyle, T.C., Coquoz, O., Kalish, F., Rice, B.W., and Contag, C.H. (2005). Emission spectra of bioluminescent reporters and interaction with mammalian tissue determine the sensitivity of detection in vivo. J. Biomed. Opt. *10*, 41210.
19. Iwano, S., Sugiyama, M., Hama, H., Watakabe, A., Hasegawa, N., Kuchimaru, T., Tanaka, K.Z., Takahashi, M., Ishida, Y., Hata, J., et al. (2018). Single-cell bioluminescence imaging of deep tissue in freely moving animals. Science *359*, 935–939.
20. Si, X., Xiao, L., Brown, C.E., and Wang, D. (2022). Preclinical Evaluation of CAR T Cell Function: In Vitro and In Vivo Models. Int. J. Mol. Sci. *23*, 3154.
21. Ong, C.S., Zhou, X., Han, J., Huang, C.Y., Nashed, A., Khatri, S., Mattson, G., Fukunishi, T., Zhang, H., and Hibino, N. (2018). In vivo therapeutic applications of cell spheroids. Biotechnol. Adv. *36*, 494–505.
22. Boucherit, N., Gorvel, L., and Olive, D. (2020). 3D Tumor Models and Their Use for the Testing of Immunotherapies. Front. Immunol. *11*, 603640.
23. Jedema, I., van der Werff, N.M., Barge, R.M.Y., Willemze, R., and Falkenburg, J.H.F. (2004). New CFSE-based assay to determine susceptibility to lysis by cytotoxic T cells of leukemic precursor cells within a heterogeneous target cell population. Blood *103*, 2677–2682.
24. Lyons, A.B. (2000). Analysing cell division in vivo and in vitro using flow cytometric measurement of CFSE dye dilution. J. Immunol. Methods *243*, 147–154.
25. Horan, P.K., and Slezak, S.E. (1989). Stable cell membrane labelling. Nature *340*, 167–168.
26. Chudakov, D.M., Matz, M.V., Lukyanov, S., and Lukyanov, K.A. (2010). Fluorescent proteins and their applications in imaging living cells and tissues. Physiol. Rev. *90*, 1103–1163.
27. Chen, K., Chen, L., Zhao, P., Marrero, L., Keoshkerian, E., Ramsay, A., and Cui, Y. (2005). FL-CTL assay: fluorolysometric determination of cell-mediated cytotoxicity using green fluorescent protein and red fluorescent protein expressing target cells. J. Immunol. Methods *300*, 100–114.
28. Zanoni, M., Piccinini, F., Arienti, C., Zamagni, A., Santi, S., Polico, R., Bevilacqua, A., and Tesei, A. (2016). 3D tumor spheroid models for in vitro therapeutic screening: a systematic approach to enhance the biological relevance of data obtained. Sci. Rep. *6*, 19103.
29. Ansari, N., Müller, S., Stelzer, E.H.K., and Pampaloni, F. (2013). Quantitative 3D cell-based assay performed with cellular spheroids and fluorescence microscopy. Methods Cell Biol. *113*, 295–309.

30. Pampaloni, F., Ansari, N., and Stelzer, E.H.K. (2013). High-resolution deep imaging of live cellular spheroids with light-sheet-based fluorescence microscopy. Cell Tissue Res. *352*, 161–177.

31. Tung, J.K., Berglund, K., Gutekunst, C.A., Hochgeschwender, U., and Gross, R.E. (2016). Bioluminescence imaging in live cells and animals. Neurophotonics *3*, 025001.

32. Troy, T., Jekic-McMullen, D., Sambucetti, L., and Rice, B. (2004). Quantitative comparison of the sensitivity of detection of fluorescent and bioluminescent reporters in animal models. Mol. Imag. *3*, 9–23.

33. Billinton, N., and Knight, A.W. (2001). Seeing the wood through the trees: a review of techniques for distinguishing green fluorescent protein from endogenous autofluorescence. Anal. Biochem. *291*, 175–197.

34. Weissleder, R. (2010). Molecular Imaging: Principles and Practice. In Functional Imaging Using Bioluminescent Markers, C.H. Contag, ed. (People's Medical Publishing House).

35. Close, D.M., Xu, T., Sayler, G.S., and Ripp, S. (2011). Ripp, In vivo bioluminescent imaging (BLI): noninvasive visualization and interrogation of biological processes in living animals. Sensors *11*, 180–206.

36. Kim, J.E., Kalimuthu, S., and Ahn, B.C. (2015). In vivo cell tracking with bioluminescence imaging. Nucl. Med. Mol. Imaging *49*, 3–10.

37. Liang, Y., Walczak, P., and Bulte, J.W.M. (2012). Comparison of red-shifted firefly luciferase Ppy RE9 and conventional Luc2 as bioluminescence imaging reporter genes for in vivo imaging of stem cells. J. Biomed. Opt. *17*, 016004.

38. Bajgain, P., Tawinwung, S., D'Elia, L., Sukumaran, S., Watanabe, N., Hoyos, V., Lulla, P., Brenner, M.K., Leen, A.M., and Vera, J.F. (2018). CAR T cell therapy for breast cancer: harnessing the tumor milieu to drive T cell activation. J. Immunother. Cancer *6*, 34.

39. Watanabe, N., Bajgain, P., Sukumaran, S., Ansari, S., Heslop, H.E., Rooney, C.M., Brenner, M.K., Leen, A.M., and Vera, J.F. (2016). Fine-tuning the CAR spacer improves T-cell potency. OncoImmunology *5*, e1253656.

40. Barrett, D.M., Zhao, Y., Liu, X., Jiang, S., Carpenito, C., Kalos, M., Carroll, R.G., June, C.H., and Grupp, S.A. (2011). Treatment of advanced leukemia in mice with mRNA engineered T cells. Hum. Gene Ther. *22*, 1575–1586.

41. Porter, D.L., Levine, B.L., Kalos, M., Bagg, A., and June, C.H. (2011). Chimeric antigen receptor-modified T cells in chronic lymphoid leukemia. N. Engl. J. Med. *365*, 725–733.

42. Li, W., Ding, L., Shi, W., Wan, X., Yang, X., Yang, J., Wang, T., Song, L., Wang, X., Ma, Y., et al. (2023). Safety and efficacy of co-administration of CD19 and CD22 CAR-T cells in children with B-ALL relapse after CD19 CAR-T therapy. J. Transl. Med. *21*, 213.

43. Leen, A.M., Sukumaran, S., Watanabe, N., Mohammed, S., Keirnan, J., Yanagisawa, R., Anurathapan, U., Rendon, D., Heslop, H.E., Rooney, C.M., et al. (2014). Reversal of tumor immune inhibition using a chimeric cytokine receptor. Mol. Ther. *22*, 1211–1220.

44. Bajgain, P., Torres Chavez, A.G., Balasubramanian, K., Fleckenstein, L., Lulla, P., Heslop, H.E., Vera, J., and Leen, A.M. (2022). Secreted Fas Decoys Enhance the Antitumor Activity of Engineered and Bystander T Cells in Fas Ligand-Expressing Solid Tumors. Cancer Immunol. Res. *10*, 1370–1385.

45. Ahmed, N., Salsman, V.S., Yvon, E., Louis, C.U., Perlaky, L., Wels, W.S., Dishop, M.K., Kleinerman, E.E., Pule, M., Rooney, C.M., et al. (2009). Immunotherapy for osteosarcoma: genetic modification of T cells overcomes low levels of tumor antigen expression. Mol. Ther. *17*, 1779–1787.

46. Richman, S.A., Nunez-Cruz, S., Moghimi, B., Li, L.Z., Gershenson, Z.T., Mourelatos, Z., Barrett, D.M., Grupp, S.A., and Milone, M.C. (2018). High-Affinity GD2-Specific CAR T Cells Induce Fatal Encephalitis in a Preclinical Neuroblastoma Model. Cancer Immunol. Res. *6*, 36–46.

47. Rivière, I., Brose, K., and Mulligan, R.C. (1995). Effects of retroviral vector design on expression of human adenosine deaminase in murine bone marrow transplant recipients engrafted with genetically modified cells. Proc. Natl. Acad. Sci. USA *92*, 6733–6737.